Molecular Crystals and Liquid Crystals
Publication details, including instructions for authors and subscription information:
http://www.tandfonline.com/loi/gmcl20

Effects of the Concentration of MgO in the Catalyst on the Growth of Carbon Nanotubes

Ming-Ji Li [a], Jia Sun [a], Hong-Ji Li [b], Bao-Kun Huang [c] & Bao-He Yang [a]

[a] Tianjin Key Laboratory of Film Electronic and Communicate Devices, School of Electronics Information Engineering, Tianjin University of Technology, Tianjin, China

[b] Chemistry and Chemical Engineering of Tianjin University of Technology, Tianjin, China

[c] Dalian Institute of Chemical Physics, Chinese Academy of Sciences, Dalian, China

Version of record first published: 16 Nov 2012.

To cite this article: Ming-Ji Li , Jia Sun , Hong-Ji Li , Bao-Kun Huang & Bao-He Yang (2012): Effects of the Concentration of MgO in the Catalyst on the Growth of Carbon Nanotubes, Molecular Crystals and Liquid Crystals, 569:1, 1-9

To link to this article: http://dx.doi.org/10.1080/15421406.2012.688404

Mol. Cryst. Liq. Cryst., Vol. 569: pp. 1–9, 2012

ISSN: 1542-1406 print/1563-5287 online
DOI: 10.1080/15421406.2012.688404

Effects of the Concentration of MgO in the Catalyst on the Growth of Carbon Nanotubes

MING-JI LI,[1] JIA SUN,[1] HONG-JI LI,[2] BAO-KUN HUANG,[3] AND BAO-HE YANG[1,*]

[1]Tianjin Key Laboratory of Film Electronic and Communicate Devices, School of Electronics Information Engineering, Tianjin University of Technology, Tianjin, China
[2]Chemistry and Chemical Engineering of Tianjin University of Technology, Tianjin, China
[3]Dalian Institute of Chemical Physics, Chinese Academy of Sciences, Dalian, China

Carbon nanotubes (CNTs) were prepared on Si substrate by radio frequency plasma-enhanced chemical vapor deposition with Ni/MgO as catalyst. The morphology and microstructure of CNTs were characterized by X-ray diffraction, scanning electron microscopy, Raman spectroscopy, and transmission electron microscopy. The results show that with increasing MgO concentration in the catalyst the diameter of CNTs becomes smaller and more uniform and their purity and crystallinity are improved. Open or close carbon nano-onion structure is formed at the top of the CNTs, and the catalyst particles are found inside the tubes. With increasing MgO concentration, nanoparticles tend to nanowires longer than 30 nm for MgO concentration of 75% in the catalyst compund. These nanowires are made by Ni. Besides, when MgO concentration is 50%, the graphite layer of the bending tube wall extends inside of the tube, dividing the cavity into several irregularly shaped spaces, which forms a new carbon nanostructure.

Keywords Carbon nanotubes; carbon nano-onion; MgO; Ni; RF-PECVD

1. Introduction

Carbon nanotubes (CNTs) [1] and carbon nano-onions [2] were discovered in early 1990s. Because of their outstanding electronic, thermal, and mechanical properties, CNTs exhibit great potential in various applications, such as electron field emitter displays, nanoscale electronic devices, fuel cell electrodes, and biosensors [3–7]. The prevalent synthesis methods include arc-discharge [8], laser ablation [9], and chemical vapor deposition (CVD) [10–12]. CVD is a low-cost, and easy-to-control technique with a higher growth rate. Radio frequency plasma-enhanced CVD (RF-PECVD) equipment, in particular, can generate a uniform plasma owing to the RF power applied between the upper and lower electrodes,

*Address correspondence to Bao-He Yang, Tianjin Key Laboratory of Film Electronic and Communicate Devices, School of Electronics Information Engineering, Tianjin University of Technology, Tianjin 300384, China. Tel.: +86 022 60215346. E-mail: bhyang207@gmail.com

and hence can prepare more uniform and better-quality CNTs, and is more suitable for large-scale preparation of CNTs.

Ni [13], Co [14], and Fe [15] and other transition metals are commonly used as catalysts for CNTs synthesis. The dimension and surface properties of the catalyst affects the CNTs synthesis directly. The preparation method of the catalysts is the key factor to the properties of the catalyst. Catalyst film is usually prepared by spin coating [16], evaporation [17], and sputtering [13], but in industrial production of CNTs, we need to consider the practical issues such as the cost. In addition, using Fe-, Ni-, and Co-containing volatile metal salts as catalyst precursors, and SiO_2 [18], Al_2O_3 [19,20], MgO [15], etc., as catalyst supports, we can obtain catalyst particles through pyrolysis and reduction processes in the hydrogen plasma in the CVD system. The catalyst supports can prevent aggregation of catalyst particles on the support surface, which is favorable for controlling the size and distribution of the catalyst particles, and for achieving uniform and small CNTs. Compared with other preparation techniques of catalysts, this method has the advantage of simplicity, low cost, and compatibility with microelectronics technology.

In this paper, we use MgO as catalyst support to prepare CNTs. Magnesium nitrate ($Mg(NO_3)_2$) has a low decomposition temperature, and we can easily blend it with the catalyst metal salt to make a mixed solution, which can be decomposed to uniformly dispersed catalyst/support mixture at 650°C, and through a simple acid treatment it can be easily removed. Some researchers investigated the catalyst system with MgO as the support, but their catalyst system was all mixed with Mo and other metals [15,21–23]. Some researchers prepared CNTs directly on the Ni/MgO compounds [24]. In this work, however, we used $Ni(NO_3)_2$ and $Mg(NO_3)_2$ as catalyst precursors. Ni/MgO compounds were produced through pyrolysis and reduction of these precursors, in the hydrogen plasma by RF-PECVD method, after which CNTs were prepared on the Ni/MgO compounds. CH_4 was adopted as carbon source to prepare CNTs. By changing the concentration of MgO, we studied the effects of MgO on the purity, crystallinity, and microstructure of CNTs.

2. Experimental

CNT on silicon (Si) wafer were grown by the RF-PECVD technique, $Ni(NO_3)_2$ and $Mg(NO_3)_2$ as the catalyst precursors. Substrates used for CNT growths were single crystal n-type Si (111) wafers and were cut into 10 × 10 mm squares. The substrates had been ultrasonically cleaned for 15 min by acetone, ethanol, and deionized water. Then $Ni(NO_3)_2{\cdot}6H_2O$ and $Mg(NO_3)_2{\cdot}6H_2O$ were dissolved into ethanol. The concentration of $Ni(NO_3)_2$ was kept constant at 0.1mol L^{-1}, while the mole fraction of MgO was set to be 0%, 25%, 50%, and 75%. The catalyst-containing solution was sprayed on the Si wafer. The wafers were dried at 80°C, and were put on the stage in the RF-PECVD equipment.

Hydrogen gas with a flow rate of 40 mL min^{-1} was introduced into the reaction chamber, and the pressure in the reaction chamber was maintained at 300 Pa. RF of 200 W was applied generating hydrogen plasma between the electrode and the sample stage. Meanwhile, the sample stage was heated up to 650°C and maintained for 30 min. The catalyst precursor decomposed into NiO and MgO at high temperature. After that, NiO was reduced into Ni nanoparticles by the hydrogen plasma. The catalyst resulting from this procedure is designated as Ni/MgO catalyst. This procedure was followed by the growth of CNTs with introducing methane. The gas flow rate of methane is 40 mL min^{-1}, and time of growth is 30 min. The purity is 99.95% for hydrogen, and 99.99% for methane. The gas flows were controlled by mass flow controllers. The temperature of the substrate was controlled by an automatic temperature control system with an accuracy of ±1°C.

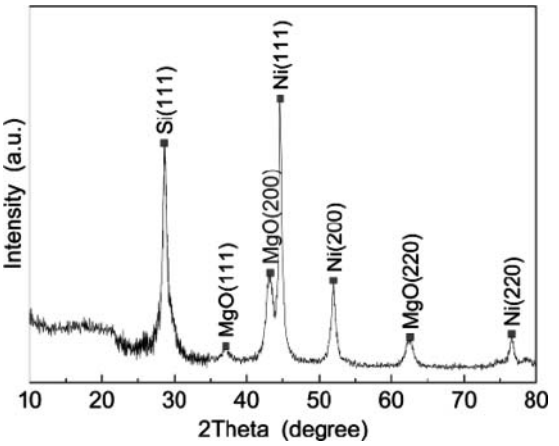

Figure 1. XRD pattern of the Ni/50% MgO catalyst precursor after reaction products by hydrogen plasma at 650°C for 30 min.

X-ray diffraction (XRD, Rigaku D/max-2500/PC) was used to study the reduction result of the catalyst precursor. The morphology, microstructure, and composition of the CNTs were characterized by scanning electron microscopy (SEM, JSM-6700F), high-resolution transmission electron microscopy (HRTEM, JEM-2100), and Raman spectroscopy (Renishaw Invia).

3. Results and Discussion

Figure 1 shows the XRD pattern of Ni/50% MgO catalyst precursor after 30 min of reduction by hydrogen plasma. XRD results only show the peaks of Si, Ni, and MgO, which indicates that at the temperature of 650°C $Ni(NO_3)_2$ and $Mg(NO_3)_2$ will completely break down to NiO and MgO, and NiO was all reduced to Ni particles after being treated by hydrogen plasma for 30 min, while MgO cannot be reduced owing to the stronger activity of Mg atoms than that of H atoms.

Figure 2 shows SEM images of the products prepared with different molar fractions of MgO. Without MgO as catalyst support, the CNTs could not be produced, and only catalyst particles and carbon particles were found on the substrate (Fig. 2a). If the catalyst particle size is greater than the critical size, the tube structure could not be formed [25]. When the content of MgO is 25%, CNTs grow, but the amount is limited, and the diameter distribution is not uniform—in the range of 10–60 nm (Fig. 2b). When the content of MgO is 50%, more CNTs grow, and the diameter range is narrower—from 10 nm to 20 nm, which is relatively uniform, but it also shows a greater amount of impurities (Fig. 2c). When the content of MgO is 75%, CNTs prepared have higher purity, and the diameters range is even narrower—at ∼10 nm (Fig. 2d). In summary, with increasing MgO content the diameter of CNTs becomes smaller, and tends to be more uniform. It can also be found in the SEM images that most of the CNTs have catalyst particles on top with the MgO content of 25%, 50%, and 75%. The growth follows a "tip-growth" mechanism when the particle is lifted over the substrate and is observed at the top of the CNTs [26]. It shows that, tip growth mechanism is likely to be responsible for the CNT synthesis under the present conditions.

During the processes of the decomposition of catalyst precursor and the reduction by hydrogen plasma, the uniform distribution of the catalyst precursor will prevent the

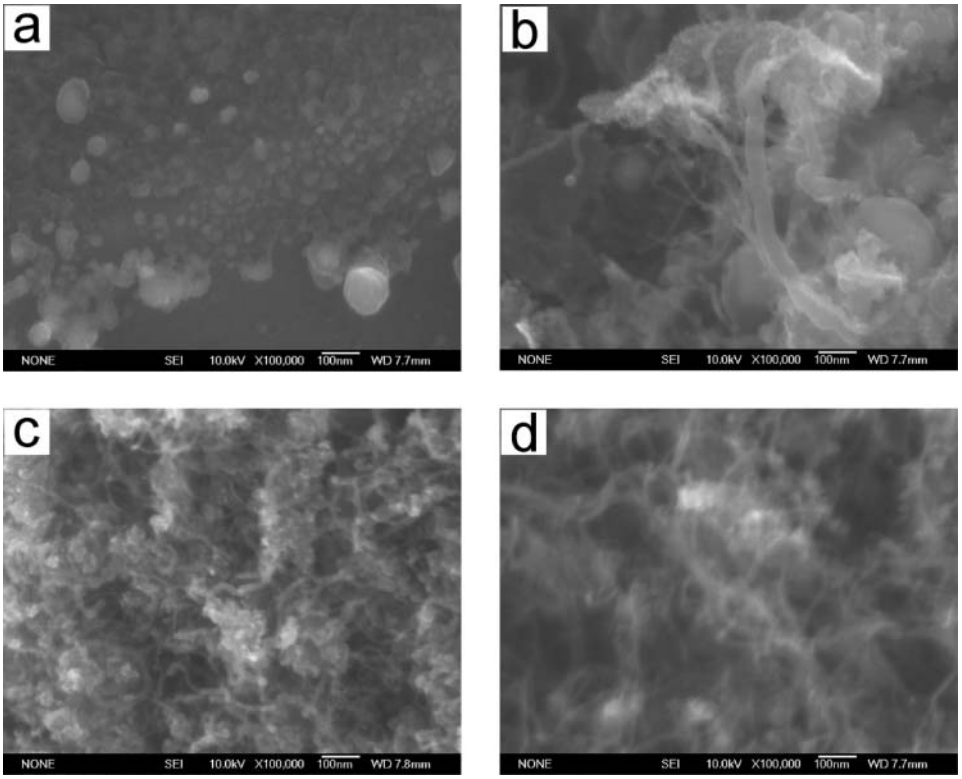

Figure 2. SEM images of the CNTs with MgO molar content of (a) 0%, (b) 25%, (c) 50%, and (d) 75%.

aggregation of Ni particles, which will then control the size of Ni particles effectively. CNTs were produced by RF-PECVD method with MgO as catalyst support. In our experimental conditions, the higher concentration of MgO results in more uniform distribution of Ni particles. And the diameter of CNTs largely depends on the size and distribution of Ni particles [27], and it becomes smaller and more uniform with increasing MgO.

Raman spectroscopy is a very effective technique for characterizing the quality of CNTs. Figure 3 shows the Raman spectra of CNTs grown by Ni/MgO catalyst. The mole fraction of MgO on different catalysts was controlled at 0%, 25%, 50%, and 75%. The spectrum shows two bands at around 1348 cm^{-1} and 1579 cm^{-1}. The bands at around 1348 cm^{-1} correspond to polycrystalline graphite and disordered carbon (D-band). The other band at around 1579 cm^{-1} is related with one of the E2g modes of single crystalline graphite (G-band). The SEM images shows that without MgO catalyst support, there are no CNTs grown, but some carbonaceous and graphite on the Ni particles (Fig. 3a). In general, the intensity ratio of D-peak and G-peak (ID/IG) can be used to evaluate the quality and crystallinity of CNTs. Lower ratio of ID/IG indicates higher purity and crystallinity of CNTs. Figure 3 also shows that the ratio rapidly decreases with increasing MgO content, which indicates that higher mole fraction of MgO results in higher purity and better crystallinity of CNTs. The Raman results agree well with SEM results.

Figure 4 shows the transmission electron microscopy (TEM) images of CNTs prepared with Ni/25% MgO as catalyst. It can be seen that carbon nano-onions show up with a small

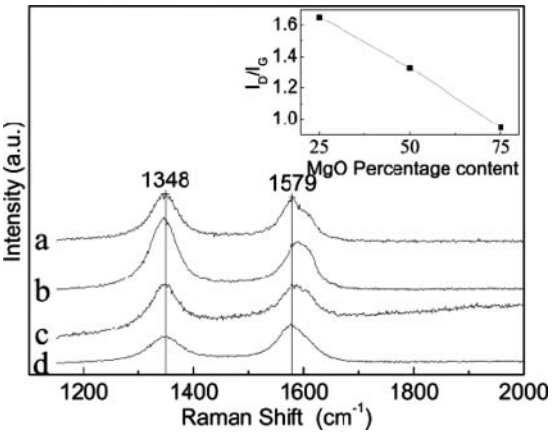

Figure 3. Raman spectra of the CNTs with MgO molar content of (a) 0%, (b) 25%, (c) 50%, and (d) 75%.

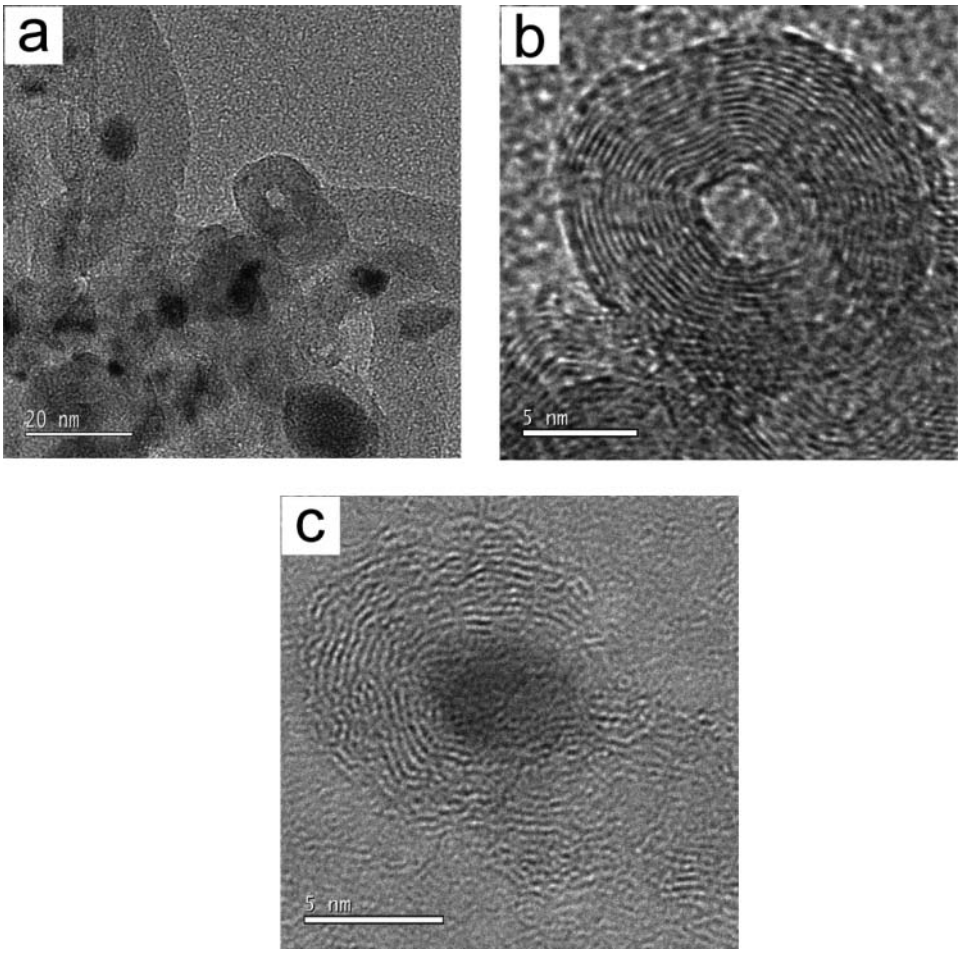

Figure 4. TEM images of the carbon nanostructure with MgO molar content of 25%.

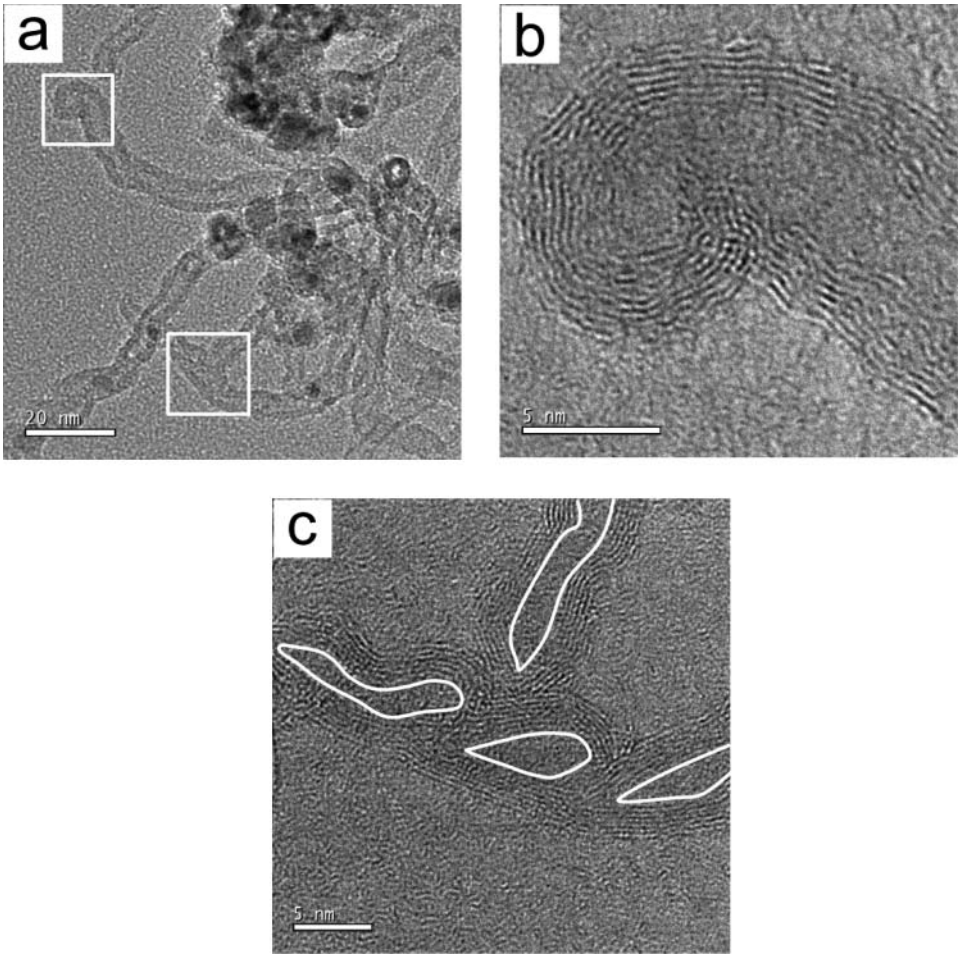

Figure 5. TEM images of the carbon nanostructure with MgO molar content of 50%.

amount of CNTs under this condition. Some carbon nano-onions grow with nanoparticles, while others without. And some nanoparticles still remain at the end or in the hollow part of the tubes (Fig. 4a). The HRTEM images of opening carbon nano-onions are shown in Fig. 4(b). Every concentric circles of a carbon nano-onion are complete and neat without fracture and without nanoparticle in the center. The nano-onion consists of 18 graphitic layers with the interlayer spacing of 0.339 nm. And the inner diameter is 3.5 nm, and the outer 15.7 nm. The ratio of outer diameter to the inner diameter is relatively big, about 4.5. In addition, carbon nano-onions form at the top of some CNTs (Fig. 4c), where the catalyst particles are completely surrounded by graphite layers, and these graphite layers are not continuous indicating they have defects.

Figure 5 shows the TEM images of CNTs with Ni/50% MgO as catalyst. The samples show hollow tubular structure, and at the top of most CNTs, curved hollow, and closed carbon onions appear. Many catalyst particles exist in the stem region, the outer and inner diameter is more uniform, and the ratio of the outer diameter to the inner diameter is about 2.5 (Fig. 5a). The hollow closed carbon onion structure in the HRTEM images shows nine

graphite layers and the tube walls were remarkably well graphitized compared with CNTs prepared with Ni/25% MgO (Fig. 4c), which indicates fewer amorphous carbon and other defectives on the tube walls (Fig. 5b). And the HRTEM images of the stem region show that one side of the graphite layer of CNTs is straight and without fracture, while the other side is bent or discontinuous forming wave-like bent tube structure (Fig. 5c). The curved graphite layer of the tube wall extends inside the tube dividing the tube cavity into several irregular spaces. This is a new structure of CNTs, which is referred to as wave-like structure. Wave-like structures form the sidewalls of CNTs in our study, and they are topologically similar to the so-called bamboo-like structures [28] and nanoprotrusions [29]. The bamboo-shaped CNTs have no encapsulated catalytic particles at the closed tip, and the compartment layers' curvature is oriented to the tip. The conical-shaped compartment layers appear periodically. Thus, the growth of bamboo-shaped CNTs follows the base growth mechanism [28]. The nanoprotrusions have closed and symmetric structure. They are formed through the catalytic opening of nanotube sidewalls. The resultant vacancy defect with dangling bonds in the CNT sidewall then becomes a center for nucleation and growth of a nanoprotrusion [29].

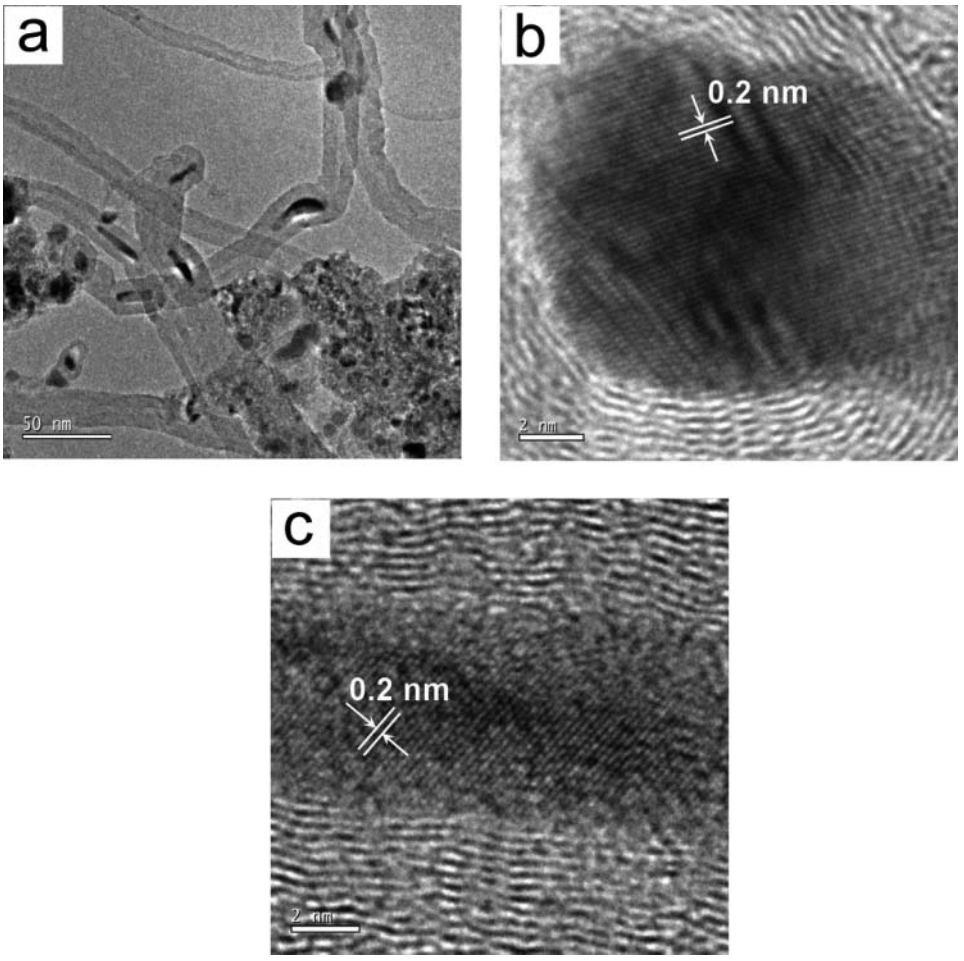

Figure 6. TEM images of the CNTs prepared with MgO molar content of 75%.

For the wave-like structures, the morphology of the internal graphite layers is similar to bamboo-like structures. And the morphology of the external side of the wall is similar to nanoprotrusion. We are looking forward to check the exciting novel properties of this new structure.

Figure 6 shows the TEM images of CNTs with Ni/75% MgO as catalyst. It can be seen that the graphite sheets of CNTs have a high degree of neatly arranged structure. The ratio of outer diameter to the inner diameter is about 5. The CNTs in this case have fewer defects, better crystallinity, and more catalyst particles in stem region (in some cases, nanowires as long as 30 nm are formed), compared with the CNTs grown with Ni/50% MgO as catalyst (Fig. 6a). Moreover, at the top of the some CNTs open carbon onions with catalyst particles inside show up.

Its crystal planes can be clearly seen in the HRTEM (Fig. 6b), and the spacing was 0.2 nm, which corresponds to the (111) crystal planes of Ni with a face-centered cubic structure. The spacing was 0.2 nm for the nanowires in the stem region of CNTs (Fig. 6c), which still corresponds to the same Ni structure, indicating that the nanowires are formed by the metal Ni.

Comparing the TEM images of the samples with different MgO contents, we found out that with increasing MgO content, catalyst Ni in the CNTs gradually increases, and has a trend of transforming from nanoparticles to nanowires. The wall of CNTs becomes more complete, and has less structural defects, and better crystallinity. These results agree well with the Raman results.

4. Conclusions

In this paper, we dissolved $Ni(NO_3)_2$ and $Mg(NO_3)_2$ into ethanol as a catalyst precursor. And in the RF-PECVD system, we used high-temperature decomposition and hydrogen plasma reduction to obtain Ni/MgO catalyst, and then prepared carbon nanostructures based on CNTs. We changed the mole fraction of MgO in the catalyst, found out that the content of MgO plays an important role in the growth of CNTs. First, as the concentration of MgO increases, the carbon nano-onions tend to become CNTs, and the top of most of CNTs presents a carbon-onion structure. Second, adding MgO appropriately, we can get a new structure of CNTs—one side of the graphite layer of CNTs is straight and without fracture, while the other side extends inside the tube dividing the tube cavity into several irregular spaces. In addition, MgO can promote the filling of metal Ni into the CNTs, and even promote the form of nanowires. By further optimizing the process, we can get a new material of CNTs filled with Ni nanowires, which might have potential applications in data storage and xerography techniques.

Acknowledgments

This work was supported by the National Natural Science Foundation of China (50972105); the Natural Science Foundation of Tianjin (08JCZDJC22700); and key project of Tianjin Education Commission (2008ZD06).

References

[1] Iijima, S. (1991). *Nature*, *354*, 56.
[2] Ugarte, D. (1992). *Nature*, *359*, 707.
[3] Slobodian, P., Riha, P., Lengalova, A., & Saha, P. (2011). *J. Mater. Sci.*, *46*, 3186.

[4] Wu, C. X., Li, F. S., Zhang, Y. A., Guo, T. L., Qu, B., & Chen, Z. J. (2011). *Appl. Surf. Sci.*, *257*, 4539.
[5] Ding, L., Wang, Z. X., Pei, T., Zhang, Z. Y., Wang, S., Xu, H. L., Peng, F., Li, Y., & Peng, L. M. (2011). *Acs. Nano.*, *5*, 2512.
[6] Park, S., Shao, Y. Y., Kou, R., Viswanathan, W., Towne, S. A., Rieke, P. C., Liu, J., Lin, Y. H., & Wang, Y. (2011). *J. Electrochem. Soc.*, *158*, 297.
[7] Pang, X., Imin, P., Zhitomirsky, I., & Adronov, A. (2010). *Macromolecules*, *43*, 10376.
[8] Kiadehi, A. D., Jahanshahi, M., Mozdianfard, M. R., Vakili-Nezhaad, G. H. R., & Seresht, R. J. (2011). *J. Exp. Nanosci.*, *6*, 432.
[9] Harris, P. J. F. (2007). *Carbon*, *45*, 229.
[10] Ionescu, M. I., Zhang, Y., Li, R. Y., Sun, X. L., Abou-Rachid, H., & Lussier, L. S. (2011). *Appl. Surf. Sci.*, *257*, 6843.
[11] Liu, H., Zhang, Y., Li, R. Y., Sun, X. L., Wang, F. P., Ding, Z. F., Mérel, P. P., & Desilets, S. V. (2010). *Appl. Surf. Sci.*, *256*, 4692.
[12] Li, L. C., & Lafdi, K. (2011). *J. Mater. Sci.*, *46*, 7328.
[13] Atthipalli, G., Epur, R., Kumta, P. N., Yang, M. J., Lee, J. K., & Gray, J. L. (2011). *J. Phys. Chem. C.*, *115*, 3534.
[14] Wang, B., Yang, Y. H., Li, L. J., & Chen, Y. (2009). *J. Mater. Sci.*, *44*, 3285.
[15] Dubey, P., Choi, S. K., Choi, J. H., Shin, D. H., & Lee, C. J. (2010). *J. Nanosci. Nanotech.*, *10*, 3998.
[16] Alvarez, N. T., Hamilton, C. E., Pint, C. L., Orbaek, A., Yao, J., Frosinini, A. L., Barron, A. R., Tour, J. M., & Hauge, R. H. (2010). *Acs. Appl. Mater. Inter.*, *2*, 1851.
[17] Patole, S. P., Alegaonkar, P. S., Shin, H. C., & Yoo, J. B. (2008). *J. Phys. D. Appl. Phys.*, *41*, 155311.
[18] Noda, L. K., Goncalves, N. S., Valentini, A., Probst, L. F. D., & Almeida, R. M. (2007). *J. Mater. Sci.*, *42*, 914.
[19] Xue, B., Liu, R., Huang, W. Z., Zheng, Y. F., & Xu, Z. D. (2009). *J. Mater. Sci.*, *44*, 4040.
[20] Santangelo, S., Messina, G., Faggio, G., Lanza, M., Pistone, A., & Milone, C. (2010). *J. Mater. Sci.*, *45*, 783.
[21] Valles, C., Mendoza, M. P., Maser, W. K., Martinez, M. T., Alvarez, L., Sauvajol, J. L., & Benito, A. M. (2009). *Carbon*, *47*, 998.
[22] Li, Y., Zhang, X. B., Tao, X. Y., Xu, J. M., Huang, W. Z., Luo, J. H., Luo, Z. Q., Li, T., Liu, F., Bao, Y., & Geise, H. J. (2005). *Carbon*, *43*, 295.
[23] Ni, L., Kuroda, K., Zhou, L. P., Ohta, K., Matsuishi, K., & Nakamura, J. (2009). *Carbon*, *47*, 3054.
[24] Jeong, H. J., An, K. H., Lim, S. C., Park, M. S., Chang, J. S., Park, S. E., Eum, S. J., Yang, C. W., Park, C. Y., & Lee, Y. H. (2003). *Chem. Phys. Lett.*, *380*, 263.
[25] Kukovitsky, E. F., L'vov, S. G., Sainov, N. A., Shustov, V. A., & Chernozatonskii, L. A. (2002). *Chem. Phys. Lett.*, *355*, 497.
[26] Charlier, J. C., Amara, H., & Lambin, P. (2007). *Acs Nano*, *1*, 202.
[27] Gohier, A., Ewels, C. P., Minea, T. M., & Djouadi, M. A. (2008). *Carbon*, *46*, 1331.
[28] Lee, C. J., & Park, J. H. (2001). *Carbon*, *39*, 1891.
[29] Chamberlain, T. W., Meyer, J. C., Biskupek, J., Leschner, J., Santana, A., Besley, N. A., Bichoutskaia, E., Kaiser, U., & Khlobystov, A. N. (2011). *Nature*, *3*, 732.